Hydrodynamic modes of a sheared granular flow from the Boltzmann and Navier–Stokes equations

V. Kumaran
Department of Chemical Engineering, Indian Institute of Science, Bangalore 560 012, India

(Received 8 August 2000; accepted 28 February 2001)

The initial growth rates for the hydrodynamic modes of the shear flow of a three-dimensional collection of inelastic spheres is analyzed using two models. The first is the generalized Navier–Stokes equations, derived for the shear flow of inelastic spheres using the Chapman–Enskog procedure, where the energy equation has an additional dissipation term due to inelastic collisions. The second is the solution of the linearized Boltzmann equation, where the distribution function in the base state is determined using a Hermite polynomial expansion in the velocity moments. For perturbations with variations in the velocity and gradient directions, it is found that the solutions obtained by two procedures are qualitatively similar, though there are quantitative differences. For perturbations with variations in the vorticity direction, it is found that there are qualitative differences in the predictions for the initial growth rate of the perturbations. © *2001 American Institute of Physics.* [DOI: 10.1063/1.1378789]

I. INTRODUCTION

Rapid flows of granular materials are widely encountered in nature as well as in industrial applications. A large number of chemical processes involve fluidized bed and circulating bed reactors where the particles transfer momentum and energy due to instantaneous collisions. Numerous geophysical flows such as rock slides and avalanches also involve regions where the grains are in a rapid state of motion. Dynamical descriptions for these flows are not as well developed as, for example, the Navier–Stokes equations for simple fluids. This is partly because of the complex interaction between the particles and the turbulent flow of the gas in practical applications such as fluidized beds. But even a simple system such as a collection of particles interacting with each other through inelastic hard sphere collisions exhibits many complex phenomena at the macroscopic level, such as convection rolls and pattern formation. The derivation of macroscopic dynamical equations from a knowledge of the microscopic particle dynamics remains a challenge for granular flows where the coefficient of restitution of interparticle collisions is not close to 1.

The simplest model flow that has been widely analyzed is the homogeneous shear flow of a granular material in the absence of gravity. In this case, there is a balance between the source of energy due to the macroscopic imposed flow, and the energy dissipation due to the inelastic collisions between particles. Constitutive models have been developed for this flow using methods similar to those used in the kinetic theory of gases.[1–4] In addition, there have been systematic derivations of kinetic equations up to Burnett order starting from the Boltzmann equation and using an expansion with the Knudsen number and the inelasticity of the particle collisions as the small parameters.[5,6] Sheared granular flows have also been investigated using molecular dynamics type computer simulations. While the early simulations[7–10] (for a review see Ref. 10) largely confirmed the results obtained by analytical methods, it became apparent[11–14] that there is the development of inhomogeneities and formation of clusters as the flow progresses.

In order to understand these phenomena, stability analyses of a set of model equations for the granular flow were undertaken.[15–19] These equations are similar to the Navier–Stokes equations for hard sphere gases, and assume a similar form for the transport coefficients. However, the energy equation has an additional term which represents the dissipation of energy due to inelastic collisions. Since the mean velocity depends on the spatial coordinate, it is not possible to obtain a closed form eigenvalue problem for a shear flow. Consequently, a transformation is made where the wave vector is a function of time, and the variation of the perturbation amplitude for this form of the wave vector is examined. It was found that the initial growth rate for the most unstable mode is positive.[15] At later times, it is found that the initially unstable perturbations become stable.[17] However, there are ''layering'' modes with variations in the gradient direction which are unstable even in the long time limit.

Another class of problems that has received attention recently is the homogeneous cooling state of a gas of inelastic particles.[13,20] Here, the base state is a gas of inelastic grains in which the ''temperature'' (mean square velocity of the particles) is decreasing with time due to inelastic collisions. The stability of the homogeneous state of the system is determined using a stability analysis about this cooling state. It is found that the homogeneous state is unstable due to the clustering of particles.[13] In addition, there is the inelastic collapse mechanism[20] which is also observed in these systems. Both the clustering and collapse mechanisms also exist in forced systems such as shear flows. The present study is about a steady state where there is a source of energy due to the mean shear, and energy dissipation due to inelastic collisions.

Since many of the previous studies of shear flow have been based on Navier–Stokes type equations, with the trans-

port coefficients determined using the Chapman–Enskog procedure starting from the Boltzmann equation, it is of interest to examine whether the scaling laws for the hydrodynamic modes obtained using these two models are the same. It is expected that the continuum equations can be obtained using an asymptotic analysis in the limit of small elasticity $(1-e)\ll 1$, but it is of importance to determine the interval of the parameter $(1-e)$ where they accurately reproduce the macroscopic dynamics. In the present paper, the initial growth rates of the hydrodynamic modes of the homogeneous sheared state is analyzed using the Boltzmann equation for inelastic spheres. The Boltzmann equation is more fundamental than the continuum Navier–Stokes equations, since the Navier–Stokes equations assume that the only relevant variables that determine the dynamics of the system are the mass, momentum, and energy. However, the Boltzmann equation already contains certain simplifying assumptions. The most important of these is the assumption that the pair distribution function is the product of the pair correlation function and the single particle velocity distributions before collision (assumption of molecular chaos). This assumption breaks down in very dense systems where there are correlated collisions between pairs of particles.

Since an infinite shear flow involves a linear variation in the mean velocity in the gradient direction, it is not possible to obtain an eigenvalue problem for systems with variations in the flow direction. It is necessary to use a time-dependent wave vector in the gradient direction, which is ''turning'' with the mean flow, as indicated in the analysis, in order to obtain an eigenvalue problem.[15] In the present analysis, we set the time equal to zero in the transformed wave vector to get solutions for the growth rate at zero time. For perturbations with variations in the flow direction, it is known from previous studies on the Navier–Stokes equations that though the initial growth rate indicates that the system is unstable, the system could still be stable in the long time limit. This is because a perturbation with wave vector in the flow direction will be rotated toward the gradient direction, and perturbations in this direction are stable. However, the most important result of this analysis concerns the stability of perturbations with variation in the vorticity direction perpendicular to the direction of shear, and this is not affected by the rotation of the wave vector by the mean flow. The stability of the flow in the vorticity direction perpendicular to the plane of shear is not probed by two-dimensional theories or simulations, and the presence of unstable modes in this direction indicates that studies restricted to two dimensions may not accurately capture the dynamics of three-dimensional shear flows. The stability of perturbations in the vorticity direction has not received as much attention in the literature as those in the flow and gradient directions.

First, the velocity distribution in the base state, which is the homogeneous shear flow, is calculated by solving the Boltzmann equation. An expansion in a basis set consisting of products of Hermite polynomials of the velocity components is used. The Boltzmann equation is a nonlinear equation, and it is difficult to determine the coefficients in the expansion in general. In the present case, the coefficients are determined using an expansion in the parameter $\epsilon=(1-e)^{1/2}$, and terms correct to $O(\epsilon^4)$ are retained in the expansion. The parameter $(1-e)^{1/2}$ is preferred to the traditional $(1-e^2)^{1/2}$ in the present case, because the coefficient of restitution is expressed as $e=1-\epsilon^2$, and there is no need to carry out factors of 2 in the definition of e. The relationship between the results of the two approaches for a homogeneous shear flow are given in Kumaran.[21,22]

The solution of the Boltzmann equation is obtained using an expansion in a set of basis functions, which are chosen to be Hermite polynomials in the present case. Similar calculations have been carried out for spheres at equilibrium[23,24] in the absence of flow, and it is known that the solutions for the growth rate are related to the transport coefficients close to equilibrium. It can be shown that the eigenvalues for the linearized Boltzmann equation for a conservative system are real and discrete in the limit of long wavelengths, and the eigenfunctions form an orthogonal basis set. In a homogeneous system, there are five eigenvalues which are zero, and the corresponding eigenfunctions are the mass, energy, and the three components of the momentum, which are conserved in collisions. All other eigenvalues are negative, indicating that other types of transients decay over time scales comparable to the collision frequency. If perturbations of wavelength k are imposed on the system, the eigenvalues corresponding to the two transverse components of the momentum and the energy decay proportional to k^2 indicating that they are diffusive. The eigenfunctions corresponding to the density and longitudinal momentum occur as a complex conjugate pair, where the imaginary part is proportional to k indicating propagating modes, while the real part is proportional to k^2. The effect of inelastic collisions on the initial amplification rates is examined in this analysis. The perturbations are expressed in terms of a basis set consisting of products of Hermite polynomials as before, and solved to determine the initial growth rates of the linearized Boltzmann equation. Though the number of solutions of the growth rate depends on the number of basis functions used in the expansion, it is observed that as in the case of conservative hard sphere gases, the solutions for the slowly decaying modes are insensitive to the number of basis functions used. It is expected that in an inelastic system, there will be only four solutions which have zero growth rates because energy is not conserved in collisions.

The calculation of the initial amplification rates from the generalized Navier–Stokes equations, derived from the Boltzmann equation using the Chapman–Enskog procedure by Sela and Goldhirsch,[6] is discussed in Sec. II. In Sec. III, the calculation of the distribution function at steady state for a homogeneous shear flow is discussed. This solution is used in Sec. IV to determine the initial growth rates of the linearized Boltzmann equation.

II. GENERALIZED NAVIER–STOKES EQUATIONS

The Navier–Stokes equations for sheared granular flows derived by Sela and Goldhirsch[6] are used in the present analysis. They used an expansion in the limit $\mathrm{Kn}\ll 1$ and $(1-e)\ll 1$, where the Knudsen number Kn is the ratio of the mean free path to the scale of description. Attention is re-

stricted to the dilute limit, for simplicity, where the Knudsen number is set equal to zero, and the results of Sela and Goldhirsch correct to $O(1-e)$ are incorporated. A coordinate system is chosen where the flow is along the x direction, the velocity gradient along the y direction and the vorticity vector is along the z direction. Variables with a superscript asterisk are used in the present section to denote dimensional variables, while variables without the superscript in Sec. III are scaled as specified. The Navier–Stokes mass, momentum, and energy equations for the present case are

$$\partial_t^*\rho^* + \partial_x^*(\rho^* u_x^*) + \partial_y^*(\rho^* u_y^*) + \partial_z^*(\rho^* u_z^*) = 0, \tag{1}$$

$$\rho^*(\partial_t^* u_x^* + u_x^*\partial_x^* u_x^* + u_y^*\partial_y^* u_x^* + u_z^*\partial_z^* u_x^*) = -\partial_x^* p^* + \partial_x^*\tau_{xx}^* + \partial_y^*\tau_{xy}^* + \partial_z^*\tau_{xz}^*, \tag{2}$$

$$\rho^*(\partial_t^* u_y^* + u_x^*\partial_x^* u_y^* + u_y^*\partial_y^* u_y^* + u_z^*\partial_z^* u_y^*) = -\partial_y^* p^* + \partial_x^*\tau_{yx}^* + \partial_y^*\tau_{yy}^* + \partial_z^*\tau_{yx}^*, \tag{3}$$

$$\rho^*(\partial_t^* u_z^* + u_x^*\partial_x^* u_z^* + u_y^*\partial_y^* u_z^* + u_z^*\partial_z^* u_z^*) = -\partial_z^* p^* + \partial_x^*\tau_{zx}^* + \partial_y^*\tau_{zy}^* + \partial_z^*\tau_{zz}^*, \tag{4}$$

$$\rho C_v(\partial_t^* T^* + u_x^*\partial_x^* T^* + u_y^*\partial_y^* T^* + u_z^*\partial_z^* T^*) = \partial_x^*(K^*\partial_x^* T^*) + \partial_y^*(K^*\partial_y^* T^*) + \partial_z^*(K^*\partial_z^* T^*) - p^*(\partial_x^* u_x^* + \partial_y^* u_y^* + \partial_z^* u_z^*) + \partial_x^*(L^*\partial_x^*\rho^*) + \partial_y^*(L^*\partial_y^*\rho^*) + \partial_z^*(L^*\partial_z^*\rho^*) + S^* - D^*, \tag{5}$$

where $\partial_t^* = (\partial/\partial t^*)$, $\partial_i^* = (\partial/\partial x_i^*)$, and t^* and x_i^* are the dimensional time and spatial variables, and indicial notation is used to represent the components of a vector. The number density ρ^* is the number of particles per unit volume, the stress tensor, τ_{ij}^*, is given by

$$\tau_{ij}^* = \mu^*(\partial_i^* u_j^* + \partial_j^* u_i^* - (2/3)\delta_{ij}\partial_k^* u_k^*), \tag{6}$$

the rate of dissipation of energy D^* due to inelastic collisions is

$$D^* = 4\sqrt{\pi}\rho^{*2} T^{*3/2} d^2(1-e), \tag{7}$$

the source of energy due to the mean shear is

$$S^* = -p^*\partial_i^* u_i^* + \tau_{ij}^*\partial_j^* u_i^*, \tag{8}$$

the viscosity μ^* in the dilute limit (divided by the particle mass) is

$$\mu^* = \frac{5}{16\sqrt{\pi}}\left(1 + \frac{5\epsilon^2}{12}\right)\frac{T^{*1/2}}{d^2}, \tag{9}$$

the thermal diffusivity K^* is

$$K^* = \frac{25}{32\sqrt{\pi}}\left(1 + \frac{15\epsilon^2}{16}\right)\frac{T^{*1/2}}{d^2}, \tag{10}$$

and the coefficient L^* which relates the diffusion of energy due to density gradients is

$$L^* = \frac{125}{64\sqrt{\pi}}\epsilon^2\frac{T^{*3/2}}{(\rho^* d^2)} \tag{11}$$

and $C_v = (3/2)$ is the specific heat at constant volume, and d is the diameter of a particle. In the above-mentioned equations, the temperature T^* is expressed in terms of energy per unit mass of a particle, so that it has units of the (velocity)^2, while the viscosity and thermal conductivity are also expressed per unit mass of a particle.

The equations are expressed in terms of Fourier modes in the shear and gradient directions. In order to obtain an eigenvalue problem, it is necessary to assume that the wave vectors are time dependent and ''turn'' with the mean flow,[15] and the wave vectors are chosen to be $k^*(t^*) = k^*(0)$, $l^*(t^*) = l^*(0) - \gamma^* t^* k^*(0)$, and $m^*(t^*) = m^*(0)$. The perturbations are assumed to be of the form[25]

$$\begin{aligned}
\rho^*(x^*,y^*,z^*,t^*) &= \rho_0^* + \hat{\rho}^*(t^*)\exp(\iota k^* x^* + \iota l^* y^* + \iota m^* z^*),\\
u_x^*(x^*,y^*,z^*,t^*) &= \gamma^* y^* + \hat{u}_x^*(t^*)\exp(\iota k^* x^* + \iota l^* y^* + \iota m^* z^*),\\
u_y^*(x^*,y^*,z^*,t^*) &= \hat{u}_y^*(t^*)\exp(\iota k^* x^* + \iota l^* y^* + \iota m^* z^*),\\
u_z^*(x^*,y^*,z^*,t^*) &= \hat{u}_z^*(t^*)\exp(\iota k^* x^* + \iota l^* y^* + \iota m^* z^*),\\
T^*(x^*,y^*,z^*,t^*) &= T_0^* + \hat{T}^*(t^*)\exp(\iota k^* x^* + \iota l^* y^* + \iota m^* z^*).
\end{aligned} \tag{12}$$

When attention is restricted to the initial growth rates at $t^* = 0$, the time-dependent perturbations are expressed as $\hat{\rho}^*(t^*) = \rho^{*\prime}\exp(s^* t^*)$, $\hat{u}_i^*(t^*) = u_i^{*\prime}\exp(s^* t^*)$, and $\hat{T}^*(t^*) = T^{*\prime}\exp(s^* t^*)$. When these expressions are inserted into (1), (2), (3), and (5) and linearized in the perturbations to the density, velocity, and temperature, the resulting equations are

$$s^*\rho^{*\prime} + \rho_0^*(\iota k^* u_x^{*\prime} + \iota l^* u_y^{*\prime} + \iota m^* u_z^{*\prime}) = 0, \tag{13}$$

$$\rho_0^*(s^* u_x^{*\prime} + \gamma^* u_y^{*\prime}) = -\iota k^*((1+e)/2)(\rho_0^* T^{*\prime} + \rho^{*\prime} T_0^*) - \mu^*((4/3)k^{*2} + l^{*2} + m^{*2})u_x^{*\prime} - (1/3)\mu^*(k^* l^* u_y^{*\prime} + k^* m^* u_z^{*\prime}) + \mu^*\gamma^*\iota l^*\left(\frac{T^{*\prime}}{2T_0^*}\right), \tag{14}$$

$$\rho_0^* s^* u_y^{*\prime} = -\iota l^*((1+e)/2)(\rho_0^* T^{*\prime} + \rho^{*\prime} T_0^*) - \mu^*(k^{*2} + (4/3)l^{*2} + m^{*2})u_y^{*\prime} - (1/3)(l^* k^* u_x^{*\prime} + l^* m^* u_z^{*\prime}) + \mu^*\gamma^*\iota k^*\left(\frac{T^{*\prime}}{2T_0^*}\right), \tag{15}$$

$$\rho_0^* s^* u_z^{*\prime} = -\iota m^*((1+e)/2)(\rho_0^* T^{*\prime} + \rho^{*\prime} T_0^*) - \mu^*(k^{*2} + l^{*2} + (4/3)m^{*2})u_z^{*\prime} - (1/3)(m^* k^* u_x^{*\prime} + m^* l^* u_y^{*\prime}), \tag{16}$$

$$\rho_0^* C_v s^* T^{*\prime} = -K^*(k^{*2}+l^{*2}+m^{*2})T^{*\prime} - L^*(k^{*2}+l^{*2}+m^{*2})\rho^{*\prime} - \frac{1+e}{2}\rho_0^* T_0^*(\iota k^* u_x^{*\prime} + \iota l^* u_y^{*\prime} + \iota m^* u_z^{*\prime})$$
$$+ \mu^* \gamma^{*2}\left(\frac{T^{*\prime}}{2T_0^*}\right) + 2\gamma^*\mu^*(\iota l^* u_x^{*\prime} + \iota k^* u_y^{*\prime}) - D^*\left(\frac{3T^{*\prime}}{2T_0^*} + \frac{2\rho^{*\prime}}{\rho_0^*}\right). \tag{17}$$

In Eqs. (13)–(17), the ideal gas equation of state $p^*=(1+e)\rho^* T^*/2$ has been used, and the gas constant has been set equal to 1 because the temperature is expressed in units of energy (per unit mass of the particle). The last terms on the right-hand side of (14) and (15), and the third term on the right-hand side of (17), account for the variation in the viscosity due to variations in the temperature, while the last term on the right-hand side of (17) accounts for the variation in the rate of dissipation of energy due to variations in the temperature and density.

For a system of elastic disks, Eqs. (13)–(16) have four solutions for s^*,[26]

$$s_1^* = -(\mu^*/\rho_0^*)k^{*2},$$
$$s_2^* = -(\mu^*/\rho_0^*)k^{*2},$$
$$s_3^* = -\frac{K^*}{\rho_0^* C_p}k^{*2}, \tag{18}$$
$$s_4^* = -\frac{1}{2}\left(\left(\frac{K^*(C_p-C_v)}{\rho_0^* C_p C_v} + \frac{4\mu^*}{3\rho_0^*}\right)k^{*2}\right) + \iota k^*\sqrt{(C_p/C_v)T^*},$$
$$s_5^* = -\frac{1}{2}\left(\left(\frac{K^*(C_p-C_v)}{\rho_0^* C_p C_v} + \frac{4\mu^*}{3\rho_0^*}\right)k^{*2}\right) - \iota k^*\sqrt{(C_p/C_v)T^*},$$

where (C_p/C_v), the ratio of specific heats, is 5/3 for a gas of elastic spheres. It was verified that the above-mentioned solutions are recovered both from the Navier–Stokes equations (13)–(17), and the linearized Boltzmann equation for the elastic case. The results of Eq. (18) are compared with those of the linearized Boltzmann equation in Sec. V.

III. NUMERICAL METHOD FOR STEADY VELOCITY DISTRIBUTION

The analysis is similar to that used earlier[21] for the two-dimensional shear flow of inelastic disks, and only a brief summary is provided here. In order to simplify the notation, the scaled velocity is defined as $\mathbf{u}=\mathbf{u}^*/T_0^{*1/2}$, where $\mathbf{u}^*$ is the dimensional velocity, and the "granular temperature" T_0^* is the mean square velocity scaled by the particle mass. The scaled spatial coordinates are defined as $\mathbf{x}=\mathbf{x}^*/(\rho_0^* d^2)^{-1}$, where $(\rho_0^* d^2)^{-1}$ is the magnitude of the mean free path of a particle, and ρ_0^* and d are the number density and the particle diameter, respectively. The scaled strain rate then becomes $\gamma=\gamma^*/(\rho_0^* d^2 T_0^{*1/2})$, where γ^* is the dimensional strain rate. In the dilute limit, the pair distribution function is 1 and the only independent parameter which affects the scaled distribution function is the coefficient of restitution e. The velocity distribution function, $f(\mathbf{x},\mathbf{u},t)$, is defined such that $f(\mathbf{x},\mathbf{u},t)d\mathbf{x}\,d\mathbf{u}$ is the number of particles in the differential volume $d\mathbf{x}$ about $\mathbf{x}$ in real space and $d\mathbf{u}$ about $\mathbf{u}$ in velocity space. For a steady homogeneous flow, $f(\mathbf{x},\mathbf{u},t)=F(\mathbf{u})$ is only a function of particle velocity. The conservation equation for this distribution function, for a mean flow with strain rate γ, is

$$-\gamma\frac{\partial u_y F(\mathbf{u})}{\partial u_x} = \frac{\partial_c F(\mathbf{u})}{\partial t}, \tag{19}$$

where the collision integral is given by

$$\frac{\partial_c F(\mathbf{u})}{\partial t} = \int d\mathbf{k}\int d\mathbf{u}^\dagger (e^{-2}F(\mathbf{u}_b)F(\mathbf{u}_b^\dagger) - F(\mathbf{u})F(\mathbf{u}^\dagger))\mathbf{w}\cdot\mathbf{k}, \tag{20}$$

where the pair distribution function has been set equal to 1 for a dilute granular flow. The coefficient e^{-2} in the first term in Eq. (20) accounts for the contraction of phase space due to inelastic collisions. In Eq. (20), $\mathbf{u}_b$ and $\mathbf{u}_b^\dagger$ are the velocities of a pair of particles before collision so that the post collisional velocities are $\mathbf{u}$ and $\mathbf{u}^\dagger$, $\mathbf{k}$ is the unit vector in the direction of the line joining the centers of particles at collision, $\mathbf{w}=\mathbf{u}-\mathbf{u}^\dagger$ is the velocity difference between the particles, and the above integral is carried out for $\mathbf{w}\cdot\mathbf{k}\geqslant 0$ so that the particles approach each other prior to collisions.

An expansion of the following form is assumed for the distribution function:

$$F(\mathbf{u}) = F_0(\mathbf{u})\left[1+\sum_{k=1}^{K} A_k \phi_k(\mathbf{u})\right], \tag{21}$$

where $F_0(\mathbf{u})$ is the Maxwell–Boltzmann distribution

$$F_0(\mathbf{u}) = \frac{1}{(2\pi)^{3/2}}\exp\left(-\frac{u^2}{2}\right). \tag{22}$$

The basis functions ϕ_k are chosen as products of Hermite polynomials in the velocity coordinate in the following manner. Due to the symmetry of the distribution function, it is necessary to retain only terms that satisfy $\phi_k(u_x,u_y,u_z)=\phi_k(-u_x,-u_y,u_z)$ and $\phi_k(u_x,u_y,u_z)=\phi_k(u_x,u_y,-u_z)$. Therefore, only Hermite polynomials of even order in the velocity u_z, and functions of the form $\mathrm{He}_n(u_x)\mathrm{He}_{p-n}(u_y)$ where p is even, are included. Of these functions, it is necessary to consider two functions separately,

$$\phi_{N-1} = (u_x^2+u_y^2+u_z^2-3)/\sqrt{6},$$
$$\phi_N = 1, \tag{23}$$

since these correspond to the conserved mass and energy modes. Here, N is the total number of basis functions used. A Gramm–Schmidt orthogonalization procedure is used to ensure that all the basis functions are orthonormal when the inner product is defined with the Gaussian as the weighting

function. There are a total of $N=14$ basis functions when all moments up to the fourth moment of the velocity are retained in the expansion.

The expansion is inserted into the Boltzmann equation, multiplied by $F_0(\mathbf{u})\phi_i(\mathbf{u})$ and integrated over the velocity coordinates to obtain a nonlinear vector equation of the form

$$-\gamma(H_i+G_{ij}A_j)=(M_i+L_{ij}A_j+N_{ijk}A_jA_k) \tag{24}$$

where summation is carried out over the repeated indices, the $K\times 1$ matrices $\hat{H}_i$ and M_i are

$$H_i=\int d\mathbf{u}\,\phi_i(\mathbf{u})\frac{\partial(u_yF_0(\mathbf{u}))}{\partial u_x}, \tag{25}$$

$$M_i=\int d\mathbf{u}\int d\mathbf{u}^{\dagger}\int d\mathbf{k}\,F_0(\mathbf{u})F_0(\mathbf{u}^{\dagger})(\phi_i(\mathbf{u}')-\phi^i(\mathbf{u}))\mathbf{w}\cdot\mathbf{k}, \tag{26}$$

the $K\times K$ matrices G_{ij} and L_{ij} are

$$G_{ij}=\int d\mathbf{u}\,\phi_i(\mathbf{u})\frac{\partial(F_0(\mathbf{u})u_y\phi_j(\mathbf{u}))}{\partial u_x}, \tag{27}$$

$$L_{ij}=\int d\mathbf{u}\int d\mathbf{u}^{\dagger}\int d\mathbf{k}\,F_0(\mathbf{u})F_0(\mathbf{u}^{\dagger})(\phi_j(\mathbf{u})+\phi_j(\mathbf{u}^{\dagger}))\times(\phi_i(\mathbf{u}')-\phi_i(\mathbf{u}))\mathbf{w}\cdot\mathbf{k}, \tag{28}$$

and the third order matrix N_{ijk} is

$$N_{ijk}=\int d\mathbf{u}\int d\mathbf{u}^{\dagger}\int d\mathbf{k}\,F_0(\mathbf{u})F_0(\mathbf{u}^{\dagger})\phi_j(\mathbf{u})\phi_k(\mathbf{u}^{\dagger})\times(\phi_i(\mathbf{u}')-\phi_i(\mathbf{u}))\mathbf{w}\cdot\mathbf{k}, \tag{29}$$

where $\mathbf{u}'$ and $\mathbf{u}^{\dagger\prime}$ are the velocities after an inelastic collision of particles which have precollisional velocities $\mathbf{u}$ and $\mathbf{u}^{\dagger}$, respectively, and $\mathbf{k}$ is the the unit vector along the line of centers at collision.

The solution procedure for determining the coefficients A_j is identical to that used in Kumaran.[22] An expansion is used in the parameter $\epsilon=(1-e)^{1/2}$, and corrections to the distribution function have been obtained correct to $O(\epsilon^4)$ or $(1-e)^2$ in the asymptotic expansion. Results were obtained for two sets of basis functions one consisting of 5 basis functions (which include all velocity moments up to second order) and the second consisting of 14 basis functions (which include all velocity moments up to fourth order). A comparison of the strain rate and the velocity moments obtained using these basis sets is shown in Fig. 1. It is observed that there is good agreement between the two basis sets for the dimensionless strain rate γ and the moment $\langle u_xu_y\rangle$ even when the coefficient of restitution is 0.7. However, there are systematic deviations in the anisotropy in the distribution function $\langle u_x^2-u_y^2\rangle$. The steady distribution obtained using a basis set consisting of 14 functions is used in the remainder of the analysis.

IV. HYDRODYNAMIC MODES

In the linear analysis, perturbations are imposed on the distribution function of the form

$$f(\mathbf{x},\mathbf{u},t)=F(\mathbf{u})+f'(\mathbf{x},\mathbf{u},t), \tag{30}$$

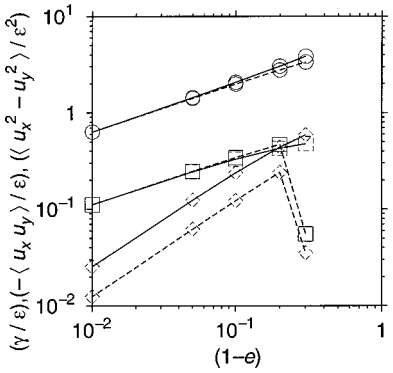

FIG. 1. The strain rate (γ/ϵ)—○, the velocity moments $(-\langle u_xu_y\rangle/\epsilon)$—△, $(\langle u_x^2-u_y^2\rangle/\epsilon^2)$—◇. The solid lines show the result for calculations with 14 basis functions, and the broken lines show the results for 5 basis functions.

where the perturbation $f'(\mathbf{x},\mathbf{u},t)$ has the form

$$f'(\mathbf{x},\mathbf{u},t)=\hat{f}(\mathbf{u},t)\exp(\iota k(t)x+\iota l(t)y+\iota m(t)z), \tag{31}$$

where $k(t)$, $l(t)$, and $m(t)$ are the time-dependent wave numbers in the x, y, and z directions, respectively,[15] and are given by

$$k(t)=k(0),\quad l(t)=l(0)-\gamma tk(0),\quad m(t)=m(0). \tag{32}$$

The above-mentioned form of the distribution function is inserted into the Boltzmann equation, and linearized about the base state to obtain an equation of the form

$$(\partial_t+\iota ku_x+\iota lu_y+\iota mu_z)\hat{f}-\gamma\frac{\partial u_y\hat{f}}{\partial u_x}=\frac{\partial_{\mathrm{cl}}\hat{f}}{\partial t}, \tag{33}$$

where the linearized collision integral is given by

$$\frac{\partial_{\mathrm{cl}}\hat{f}}{\partial t}=\int d\mathbf{u}^{\dagger}\int d\mathbf{k}(e^{-2}(F(\mathbf{u}_b)\hat{f}(\mathbf{u}_b^{\dagger})+F(\mathbf{u}_b^{\dagger})\hat{f}(\mathbf{u}_b))-F(\mathbf{u})\hat{f}(\mathbf{u}^{\dagger})-F(\mathbf{u}^{\dagger})\hat{f}(\mathbf{u}))\mathbf{w}\cdot\mathbf{k}. \tag{34}$$

Attention is restricted to the initial growth rates (at $t=0$) for arbitrary values of $(k(0),l(0),m(0))$, for which the form of the expansion is

$$\hat{f}(\mathbf{u},t)=\exp(st)\tilde{f}(\mathbf{u}), \tag{35}$$

where s is the initial growth rate. A series of the following form is assumed for the perturbation to the distribution function $\tilde{f}$,

$$\tilde{f}(\mathbf{u})=F_0(\mathbf{u})\sum_{i=1}^{K}\tilde{A}_i\phi_i, \tag{36}$$

where the basis functions ϕ_i are defined in a manner similar to that for the steady distribution, but the functions included are not restricted to even functions of u_z or those following the symmetry $f(u_x,u_y,u_z)=f(-u_x,-u_y,u_z)$. This series is inserted into Eq. (33), multiplied by the basis function $\phi_i(\mathbf{u})$, and integrated over the particle velocities to get the following matrix equation:

$$(sI_{ij}+\iota kX_{ij}+\iota lY_{ij}+imZ_{ij}-\gamma G_{ij}-C_{ij})\tilde{A}_j=M_{ij}\tilde{A}_j=0, \tag{37}$$

where I_{ij} is the identity matrix, and the other matrices are defined as

$$X_{ij}=\int d\mathbf{u}\, u_x \phi_i(\mathbf{u})\phi_j(\mathbf{u}),$$

$$Y_{ij}=\int d\mathbf{u}\, u_y \phi_i(\mathbf{u})\phi_j(\mathbf{u}),$$

$$Z_{ij}=\int d\mathbf{u}\, u_z \phi_i(\mathbf{u})\phi_j(\mathbf{u}), \tag{38}$$

$$G_{ij}=\int d\mathbf{u}\, \phi_i(\mathbf{u})\frac{\partial u_y \phi_j(\mathbf{u})}{\partial u_x},$$

$$C_{ij}=\int d\mathbf{u}\int d\mathbf{u}^{\dagger}(F(\mathbf{u})\phi_j(\mathbf{u}^{\dagger})+F(\mathbf{u}^{\dagger})\phi_j(\mathbf{u}))$$
$$\times(\phi_i(\mathbf{u}')-\phi_i(\mathbf{u}))\mathbf{w}\cdot\mathbf{k}.$$

In Eq. (38), $\mathbf{u}'$ and $\mathbf{u}^{\dagger\prime}$ are the postcollisional velocities of a pair of particles with precollisional velocities $\mathbf{u}$ and $\mathbf{u}^{\dagger}$. The dispersion relation is obtained by setting the determinant of the matrix M_{ij} equal to zero, so that there are nontrivial solutions for the amplitudes A_j.

V. RESULTS

It is first useful to analyze the results for the case of elastic particles, where there is no energy loss during collisions. For a basis set consisting of N functions, there are N solutions for s. For an elastic system, it can be shown that there are five eigenvalues with $s=0$ for a uniform system $k=0$, $l=0$, $m=0$. The corresponding eigenfunctions of the matrix M_{ij} are the mass, the three components of the momentum, and the total energy. All other eigenfunctions have negative growth rates, indicating that they decay over time scales proportional to the inverse of the collision frequency. In the long wave limit $k\to 0$, there are three diffusive modes for which the growth rate is negative and proportional to k^2. Two of these are the transverse momentum modes, which have identical decay rates, and the third is the energy mode. For the other two propagating (sound) modes, the real part of the growth rate is negative and proportional to k^2, while the imaginary parts are equal in magnitude and opposite in sign, and magnitude of the imaginary part increases proportional to k. The variation of the decay rates of the hydrodynamic modes for an elastic system are shown as a function of k in Fig. 2. It is observed that the decay rates obtained using the generalized Navier–Stokes equations and the Boltzmann equation are identical in the limit of small wave number, though there are small variations for $k\sim O(1)$. This variation is to be expected, because descriptions such as the Navier–Stokes equations are valid only in the hydrodynamic limit when the wavelength of the fluctuations is large compared to the mean free path.

A. Perturbations in the velocity direction $l=0$, $m=0$

The qualitative behavior of the hydrodynamic modes for perturbations with wave vectors in the velocity direction is similar to that reported earlier for a two-dimensional flow.[22]

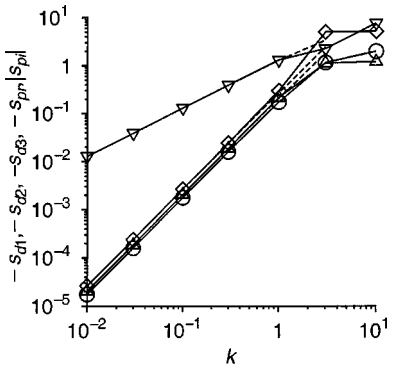

FIG. 2. The growth rates for the shear modes $s_{d1}=s_{d2}$ (○); the energy mode s_{d3} (◇), and the real s_{pr} (△) and imaginary part $|s_{pi}|$ (▽) of the growth rate of the propagating modes as a function of wave number k for an elastic system. The solid lines show the results obtained from the linearized Boltzmann equation obtained using a basis set consisting of 20 basis functions, and the broken lines show the results of the Navier–Stokes equations.

The salient features of the behavior, which is common to both the solutions of the Navier–Stokes equations as well as the Boltzmann equation, are as follows.

(1) There is one diffusive mode, which is a continuation of one of the transverse momentum modes in the elastic system, which has a positive initial growth rate in the limit $k\to 0$, and has the form

$$s_{d1}=s_{d1k}|k|^{2/3}, \tag{39}$$

where s_{d1k} is a positive coefficient. A comparison of the growth rate s_{d1} obtained from the Navier–Stokes equation and the Boltzmann equation is shown in Fig. 3. It is observed that there is good agreement for small values of k, but the initial growth rate predicted by the Navier–Stokes equation is lower than that of the Boltzmann equation for $k\sim 1$. This is consistent with the results obtained for a two-dimensional system.[22] The coefficient s_{d1k}, shown as a function of the coefficient of restitution $1-e$ in Fig. 4, decreases proportional to $(1-e)^{1/3}$ in the limit $(1-e)\to 0$. It is observed that though the qualitative behavior of this diffusive mode pre-

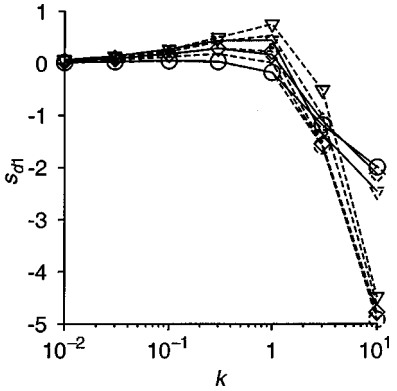

FIG. 3. The growth rate for the most unstable diffusive mode s_1 as a function of the wave vector k in the flow direction for (○) $e=0.99$, (◇) $e=0.9$, and (▽) $e=0.7$. The solid lines show the results from the Boltzmann equation, and the broken lines show the results from the Navier–Stokes equations.

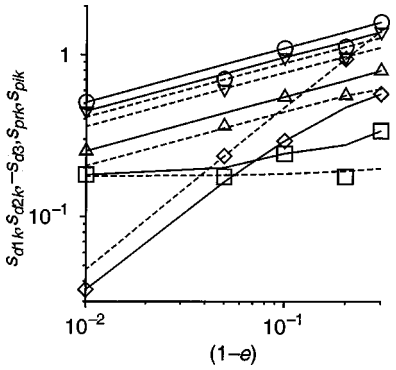

FIG. 4. The coefficients s_{d1k} (○), s_{d2k} (□), s_{prk} (△), s_{pik} (▽), and $-s_{d3}$ (◇) as a function of $(1-e)$ in the limit $k\to 0$. The solid lines show the coefficients obtained using the linearized Boltzmann equation, and the broken lines show the coefficients obtained from the generalized Navier–Stokes equations.

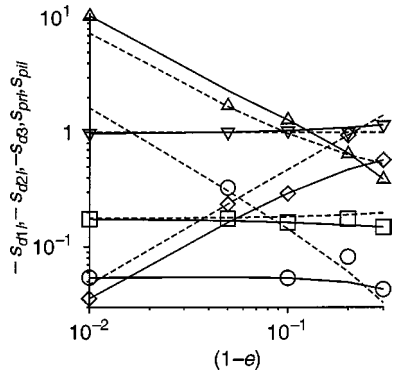

FIG. 5. The coefficients s_{d1l}, s'_{d1l} (○), s_{d2l} (□), s_{prl} (△), s_{pil} (▽), and $-s_{d3}$ (◇) as a function of $(1-e)$ in the limit $k\to 0$. The solid lines show the coefficients obtained using the linearized Boltzmann equation, and the broken lines show the coefficients obtained from the generalized Navier–Stokes equations.

dicted by the two methods are in agreement, there are is a quantitative difference of about 20 percent in the value of s_{d1k} predicted by the two methods. The analytical value of s_{d1k} can be determined from the Navier–Stokes equations in the limit $(1-e)\to 0$,

$$s_{d1k}=2^{2/3}(1-e)^{1/3}\pi^{1/6}. \tag{40}$$

(2) The second diffusive mode, which is a continuation of the second transverse momentum mode, has the form similar to that for an elastic system

$$s_{d2}=-s_{d2k}k^2. \tag{41}$$

The value of s_{d2k} obtained from the Navier–Stokes equations is identical to that for an elastic system, but the value obtained from the Boltzmann equation is not exactly the same, as shown in Fig. 4. In the limit $(1-e)\to 0$, the analytical expression for s_{d2k} from the Navier–Stokes equations is identical to that obtained for an elastic system.

$$s_{d2k}=\frac{5}{16\sqrt{\pi}}. \tag{42}$$

(3) The third diffusive mode, which is a continuation of the energy mode in elastic systems, has a finite decay rate in the limit $k\to 0$. In the limit $(1-e)\ll 1, s_{d3}\propto(1-e)$ as shown in Fig. 5. The value of s_{d3} predicted by the Navier–Stokes equations is $s_{d3}=-8(1-e)\sqrt{\pi}/3$ in the limit $(1-e)\to 0$, but the value predicted by the Boltzmann equation differs by about 20%.

(4) The real and imaginary parts of the propagating modes have the form

$$\begin{aligned} s_{pr}&=-s_{prk}|k|^{2/3},\\ s_{pi}&=\pm s_{pik}|k|^{2/3}, \end{aligned} \tag{43}$$

where s_{prk} and s_{pik} are positive, and decrease proportional to $(1-e)^{1/3}$ in the limit $1-e\ll 1$ as shown in Fig. 4. The predictions of these coefficients are also quantitatively different by the two procedures. The analytical expression for s_{prk} and s_{pik} from the Navier–Stokes equations is

$$s_{prk}=2^{-1/3}(1-e)^{1/3}\pi^{1/6}, \tag{44}$$

$$s_{pik}=3^{1/2}2^{-1/3}(1-e)^{1/3}\pi^{1/6}. \tag{45}$$

The results for the initial growth rates for the variations in the flow direction indicate that the predictions of the Navier–Stokes equation and the Boltzmann equation are qualitatively similar, but there are quantitative differences of about 20% even when the coefficient of restitution is 0.99.

B. Perturbations in the gradient direction $k=0$, $m=0$

The variation of the hydrodynamic modes with wave number l in the gradient direction is considered next. The predictions of the generalized Boltzmann equation are very similar to those for a two-dimensional system, but there are some qualitative differences in predictions of the Navier–Stokes equation.

(1) The asymptotic behavior for the least stable mode from the generalized Boltzmann equation has the usual form

$$s_{d1}=-s_{d1l}l^2, \tag{46}$$

where s_{d1l} is a positive coefficient, and this coefficient tends to a constant value in the limit $(1-e)\to 0$, as shown in Fig. 5. However, the Navier–Stokes equations provide a different form

$$s_{d1}=-s'_{d1l}l^4, \tag{47}$$

where s'_{d1l} is also a positive coefficient, but this coefficient increases proportional to $(1-e)^{-1}$ in the limit $(1-e)\to 0$, as shown in Fig. 5. The asymptotic value of s'_{d1l} from the Navier–Stokes equations is

$$s'_{d1l}=\frac{375}{4096(1-e)\pi^{3/2}}. \tag{48}$$

(2) The second diffusive mode, corresponding to one of the shear modes in an elastic system, is also stable and has the behavior

$$s_{d2}=-s_{d2l}l^2, \tag{49}$$

where s_{d2l} is a positive coefficient. The coefficients obtained from the Boltzmann equation and the Navier–Stokes equa-

TABLE I. Initial growth rates for perturbations with wave vector in the vorticity direction from the Boltzmann equation.

	$e=0.99$, $m=0.001$	$e=0.99$, $m=0.01$	$e=0.9$, $m=0.01$	$e=0.9$, $m=0.1$
s_1	1.217×10^{-3}	9.485×10^{-3}	1.166×10^{-2}	8.606×10^{-2}
s_2	3.045×10^{-5}	2.887×10^{-4}	8.707×10^{-4}	7.200×10^{-3}
s_3	-3.080×10^{5}	-2.255×10^{-2} $+9.309\times10^{-3}\iota$	-9.041×10^{-4}	-0.1930 $+0.1133\iota$
s_4	-1.309×10^{-3}	-2.255×10^{-2} $-9.309\times10^{-3}\iota$	-1.274×10^{-2}	-0.1930 -0.1133ι
s_5	-3.546×10^{-2}	-3.401	-0.2925	-2.7564

tions are in good agreement, and are identical to the value s_{d2k} for the perturbations in the velocity direction.

(3) The third diffusive mode, which is a continuation of the energy mode in an elastic system, has a negative growth rate, which attains a constant value in this limit $l\to0$, because energy is dissipated in collisions. The magnitude of the growth rate decreases proportional to $(1-e)$ in the limit $(1-e)\to0$.

(4) The real (s_{pr}) and imaginary (s_{pi}) parts of the propagating modes have the asymptotic behavior

$$s_{pr}=-s_{prl}l^2, \quad s_{pi}=\pm s_{pil}l, \tag{50}$$

where s_{prl} and s_{pil} are positive coefficients. The numerical values of the coefficients determined from the Boltzmann equation and the Navier–Stokes equations are in good agreement. The coefficient s_{prl} increases proportional to $(1-e)^{-1}$ in the limit $(1-e)\to0$, while the coefficient s_{pil} attains a finite value in this limit. The asymptotic values of s_{prl} and s_{pil} from the Navier–Stokes equations in the limit $(1-e)\to0$ are

$$s_{prl}=\frac{1}{8(1-e)\sqrt{\pi}}, \quad s_{pil}=1. \tag{51}$$

These are, however, different from the coefficients for an elastic system even when $e=0.99$.

C. Perturbations in the vorticity direction $k=0$, $l=0$

The growth rates of the hydrodynamic modes in the vorticity direction ($k=0,l=0$) show unusual behavior. For low values of the wave vector m, the growth rates of the five modes are all real, and there are no propagating modes. As the value of m is increased, there is a crossover to three real

TABLE II. Initial growth rates for perturbations with wave vector in the vorticity direction from the generalized Navier–Stokes equations.

	$e=0.99$, $m=0.001$	$e=0.99$, $m=0.1$	$e=0.9$, $m=0.01$	$e=0.9$, $m=0.3$
s_1	9.7265×10^{-4}	2.315×10^{-2}	9.718×10^{-3}	0.1507
s_2	-1.770×10^{-7}	-1.770×10^{-3}	-1.837×10^{-5}	-1.653×10^{-2}
s_3	-1.770×10^{7}	-1.770×10^{-3}	-1.837×10^{-5}	-1.653×10^{-2}
s_4	-1.029×10^{-3}	-3.861×10^{-2} $+0.1306\iota$	-1.030×10^{-2}	-0.345 $+0.379\iota$
s_5	-4.720×10^{-2}	-3.861×10^{-2} $+0.1306\iota$	-0.472	-0.345 -0.379ι

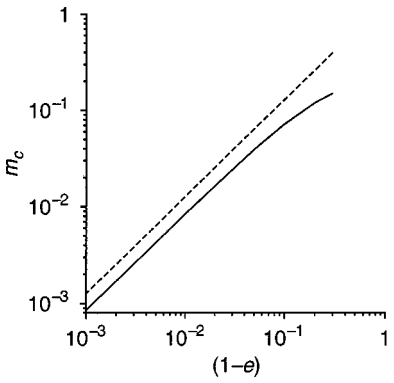

FIG. 6. Wave vector m_c for the crossover from five diffusive hydrodynamic modes to three diffusive and two propagating modes as a function of $(1-e)$. The solid lines shows the result obtained from the generalized Boltzmann equation, and the broken line shows the result obtained from the Navier–Stokes equations.

and two complex conjugate solutions for the growth rate, similar to that for an elastic system. This behavior is observed in the solutions of the Boltzmann equation, as shown in Table I, and the Navier–Stokes equations, as shown in Table II. The value of the wave number m_c at which there is a crossover from five diffusive to three diffusive and two propagating modes is shown in Fig. 6. The qualitative behavior of m_c obtained from the Boltzmann equation and Navier–Stokes equations are similar, and both methods indicate that $m_c\propto(1-e)$ for $(1-e)\to0$, but there is a quantitative difference in the prediction of the two equations. The scaling behavior of the hydrodynamic modes for variations in the vorticity direction from the Boltzmann equation are as follows. There are five diffusive modes, two of which are stable and three are unstable. One of the stable modes s_{d3}, which is a continuation of the energy mode in an elastic system, tends to a finite value in the limit $m\to0$, as shown in Fig. 7. The other four modes have the behavior

$$s_{d1}=s_{d1m}m, \tag{52}$$

$$s_{d2}=s_{d2m}m, \tag{53}$$

$$s_{d4}=-s_{d4m}m, \tag{54}$$

$$s_{d5}=-s_{d5m}m, \tag{55}$$

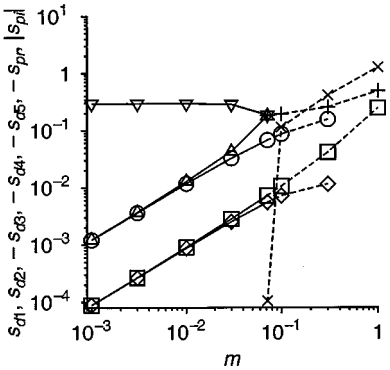

FIG. 7. The initial growth rates s_{d1} (○), s_{d2} (□), $-s_{d3}$ (▽), $-s_{d4}$ (◇), $-s_{d5}$ (△), $-s_{pr}$ (+), and $|s_{pi}|$ (×) as a function of wave number m obtained from the linearized Boltzmann equation.

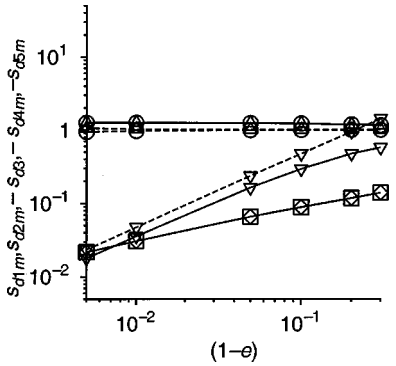

FIG. 8. The coefficients s_{d1m} (○), s_{d2m} (□), $-s_{d3}$ (▽), s_{d4m} (◇), and s_{d5m} (△) as a function of $(1-e)$ in the limit $m\to 0$.

where s_{d1m}, s_{d2m}, s_{d4m}, and s_{d5m} are positive coefficients. At the critical value m_c, the growth s_{d1}, s_{d2}, and s_{d4}, vary continuously. The growth rates s_{d3} and s_{d5} assume equal values at m_c, and give rise to two complex conjugate growth rates for $m>m_c$. The variation of the coefficients s_{d1m}, s_{d2m}, s_{d3}, s_{d4m}, and s_{d5m} are shown as a function of $(1-e)$ in Fig. 8. This figure indicates that $s_{d3}\propto(1-e)$ in the limit $(1-e)\to 0$, in agreement with the results for the velocity and strain rate directions. The coefficients s_{d1m} and s_{d5m} attain constant values in this limit, while the coefficients s_{d2m} and s_{d4m} decrease proportional to $(1-e)^{1/2}$.

Three of the growth rates determined from the Navier–Stokes equations, s_{d1}, s_{d3}, and s_{d5} are qualitatively similar to those determined from the Boltzmann equation, and there is a coalescence of the growth rates s_{d3} and s_{d5} to generate propagating modes with complex conjugate growth rates at the crossover value m_c. However, the numerical values predicted by the Navier–Stokes equations vary by about 25% from those of the predictions of the Boltzmann equation. In the limit $(1-e)\to 0$, the coefficients s_{d1m} and s_{d5m} assume the values

$$s_{d1m}=1, \tag{56}$$

$$s_{d5m}=1, \tag{57}$$

while the growth rate for the energy mode s_{d3} converges to the value

$$s_{d3}=-\frac{8(1-e)\sqrt{\pi}}{3}. \tag{58}$$

However, the predictions of the Navier–Stokes equations are qualitatively different. The growth rates s_{d1} and s_{d5} are qualitatively similar to those predicted by the Boltzmann equation, but there are numerical differences. However, the growth rates s_{d2} and s_{d4} are not predicted by the Navier–Stokes equations. Instead, the Navier–Stokes equations predict two growth rates that are negative and equal, and have the value $(-5m^2/16\sqrt{\pi})$, identical to that for the shear modes in an elastic system.

VI. CONCLUSIONS

The present study attempted to examine the suitability of the generalized Navier–Stokes equations for the study of rapid granular flows. A comparison was made between the results of the generalized Navier–Stokes equations, modified to include the dissipation due to inelastic collisions, and the solution of the Boltzmann equation for the initial growth rates of the hydrodynamic modes of a three-dimensional sheared granular flow. The Boltzmann equation already contains the assumption of molecular chaos, which states that the pair distribution function is the product of single particle distribution functions for colliding particles. In addition, the dilute limit was considered, where the pair distribution function was set equal to 1. But the Boltzmann equation is more general than the Navier–Stokes equations because it is not assumed that the only relevant variables are the mass, momenta, and energy of the particles. The effect of these assumptions can be inferred from a comparison of the results of the Boltzmann and Navier–Stokes equations. For most of the comparisons, attention was restricted to the low wave number (hydrodynamic) limit, where the length scales are large compared to the mean free path, since a hydrodynamic description is only valid in this limit. The growth rates for perturbations in the velocity, gradient, and shear directions were considered.

The growth rate for perturbations in the velocity direction is very different from that for an elastic system. There is one mode, which is a continuation of one of the transverse momentum modes in an elastic system, which is unstable. The growth rate for this mode increases proportional to $k^{2/3}$ in the limit $k\to 0$, where k is the wave vector of the perturbations in the velocity direction. The continuation of the propagating modes are stable, but their real and imaginary parts are also proportional to $k^{2/3}$ in the limit $k\to 0$. The $|k|^{2/3}$ behavior of the diffusive modes is also observed in other systems where there is a large velocity gradient. For example, in ''thermostated'' sheared hard sphere gases, where each molecule experiences a drag force proportional to its velocity, the $|k|^{2/3}$ behavior of the decay rate is observed for certain types of thermostats.[27] This is due to the ''turning'' of the wave vector by the mean shear flow, as can be seen by considering a convection-diffusion equation with mean velocity $u_x=\gamma y$,

$$\partial_t c+\partial_x(\gamma y c)=D(\partial_x^2+\partial_y^2)c, \tag{59}$$

where x and y are the gradient and flow directions, and D is the diffusion coefficient. The Fourier transform of the above equation is

$$\partial_t c+k\frac{\partial c}{\partial l}=-D(k^2+l^2)c, \tag{60}$$

where k and l are the wave vectors in the x and y directions. The solution of Eq. (60) is

$$c(k,l,t)=c_0(t)\exp[-Dt(k^2+l^2-\gamma tkl+\tfrac{1}{3}\gamma^2t^3k^2)]. \tag{61}$$

From Eq. (61), it is clear that though the behavior of the concentration field is diffusive at small times [$c\propto\exp(-Dk^2t)$], the behavior at long times in the x direction is not diffusive but is of the form [$c\propto\exp(-D\gamma^2t^3k^2/3$], which gives the decay rate proportional to $|k|^{2/3}$. However,

there are three significant differences between the behavior of a thermostatted gas and the present system.

(1) The anomalous behavior of the diffusive mode is observed only for certain types of thermostats (where the drag coefficient is a function only of the local density and temperature), but is not present in other types of thermostats (where the drag coefficient is a function of the density and temperature in the uniform flow). In the present case, this type of anomalous scaling is observed for values of the coefficient of restitution less than 0.99.

(2) The diffusive mode is stable for thermostated systems, as indicated by the solution 61, and it is one of the propagating modes which goes unstable, whereas in the present case the diffusive mode with the anomalous scaling is unstable.

(3) In diffusive systems a crossover is expected from the $s \propto k^2$ behavior at small times (high frequencies or slow driving) to the $s \propto |k|^{2/3}$ at long times (low frequencies or large driving). This crossover in inelastic particle systems occurs at $(1-e)$ in the range 10^{-3}–10^{-4}, indicating that diffusive motion is not likely to be observed for systems of practical interest.

The scaling behavior predicted by the Navier–Stokes equations are identical to those predicted by the Boltzmann equation, but the numerical values differ quantitatively by about 20%.

The initial growth rate of perturbations in the gradient direction is also similar to that for at two-dimensional system. However, there is one qualitative difference between the predictions of the Boltzmann and Navier–Stokes equations, which is the behavior of one of the stable shear modes. The Boltzmann equation predicts that the magnitude of the decay rate increases proportional to l^2, whereas the Navier–Stokes equations provide an asymptotic behavior proportional to l^4, where l is the wave number in the gradient direction. There are also quantitative differences in the predictions of the growth rates.

The initial growth rates of the perturbations in the vorticity direction show unusual behavior. At very low values of the wave number m, there are five real solutions to the initial growth rate, in contrast to the three real and two complex conjugate solutions for the velocity and gradient directions. As the wave number is increased, there is a crossover to three real and two complex conjugate solutions. The Boltzmann equation predicts that in the limit $m \to 0$, two of the solutions are positive, indicating the presence of two unstable modes. The two unstable solutions and two of the stable solutions for the growth rate vary proportional to the wave vector m in the limit $m \to 0$, while the third stable solution, which is a continuation of the energy mode in elastic systems, converges to a finite value in this limit. Three of the solutions of the Navier–Stokes equations are qualitatively similar to those of the Boltzmann equation, but the solutions for the transverse momentum modes are similar to those for an elastic system, with the difference that the viscosity now depends on the coefficient of restitution. This is because balance laws for only five velocity moments are used in the Navier–Stokes model, and the equations for the transverse momentum modes are decoupled from the mass, longitudinal momentum, and energy modes as shown in the following. When all the second moment equations are retained, there are additional couplings between equations for all the second moments resulting in a qualitatively different set of scaling relations.

The increase of the growth rate proportional to m in the limit $m \to 0$ is unusual, and does not seem to have been observed before. Whereas the scaling of the growth rate proportional to $k^{2/3}$ in the flow direction can be explained from kinematic considerations, the scaling proportional to m is due to the presence of inelastic collisions. This can be inferred by considering a simplified version of the Navier–Stokes equations for the limit $k=0$ and $l=0$. In this case, the equations for the velocities in the x and y directions decouple from those for the velocity in the z direction, and it is necessary to consider only the mass, z momentum, and energy equations,

$$s^* \rho^{*\prime} + i m^* \rho_0^* u_z^{*\prime} = 0, \tag{62}$$

$$s^* \rho_0^* u_z^{*\prime} = -i m^* T_0^* \rho^{*\prime} - i m^* \rho_0^* T^{*\prime} - \mu^* m^{*2} u_z^{*\prime}, \tag{63}$$

$$\rho_0^* C_v s^* T^{*\prime} = -K^* m^{*2} T^{*\prime} - \rho_0^* T_0^* \iota m^* u_z^{*\prime} - D^* \left(\frac{T^{*\prime}}{T_0^*} + \frac{2\rho^{*\prime}}{\rho_0^*} \right), \tag{64}$$

where $\mu^* \gamma^2 = D^*$ has been used to simplify the last two terms on the right-hand side of (17). In the limit $m^* \to 0$, one of the solutions, corresponding to the decay rate of energy fluctuations, assumes a finite value $s^* = -(D^*/\rho_0^* C_v T_0^*)$. The other two solutions which are proportional to m^* in the limit $m^* \to 0$ are real. These can be determined as follows. From Eq. (62), $u_z^{*\prime} = -(s^* \rho_{*\prime} / \iota m^* \rho_0^*)$, and if we neglect the diffusive term proportional to m^{*2} in Eq. (63), we get

$$\frac{T^{*\prime}}{T_0^*} = -\frac{\rho^{*\prime}}{\rho_0^*} \left(1 + \frac{s^{*2}}{m^{*2} T_0} \right). \tag{65}$$

This is inserted into Eq. (64) to provide, at leading order,

$$-2D^* + (\rho_0^* C_v T_0^* s^* + D^*) \left(1 + \frac{s^{*2}}{m^{*2} T_0^*} \right) = 0. \tag{66}$$

It is easily verified that due to the presence of the dissipation due to inelastic collisions, Eq. (66) provides real roots

$$s^* = \pm m^* \sqrt{T_0^*}. \tag{67}$$

Another issue of interest is the significant change in the scaling behavior when the coefficient of restitution is changed from 1.00 to 0.99, and whether this is a continuous change or a discontinuous one. For the two-dimensional system,[22] it was observed that the change is continuous, and the scalings for an elastic system are recovered for $(1-e) < 10^{-4}$. Calculations for the three-dimensional case show a similar behavior. Therefore, though the change from the usual hydrodynamic scalings to the unusual scalings reported here is gradual, it is not likely to be of practical interest since the parameter regime for the usual hydrodynamic scalings is not relevant to practical systems.

The significant result of this analysis is that perturbations in the vorticity direction show unusual behavior, and there

are qualitative differences between the predictions of the Boltzmann equation and the Navier–Stokes equations. This indicates that it is necessary to include dynamical equations of all the second moments in order to accurately capture the dynamics of the system. There are two solutions for the growth rate which are real and positive, indicating that perturbations are unstable in the vorticity direction. It should be noted that in the vorticity direction, there is no variation in the wave vector due to the rotation imposed by the shear flow, and therefore the initial growth rate is identical to that calculated using a linear analysis even at long times. Therefore, the present analysis indicates that the flow is unstable to perturbations in the vorticity direction. Since variations in the vorticity direction are not captured by two-dimensional simulations and analyses, the present analysis indicates that the dynamics of a three-dimensional shear flow could be very different from that predicted by two-dimensional studies.

[1]S. B. Savage and D. J. Jeffrey, ''The stress tensor in a granular flow at high shear rates,'' J. Fluid Mech. **110**, 255 (1981).
[2]J. T. Jenkins and S. B. Savage, ''A theory for the rapid flow of identical, smooth, nearly elastic particles,'' J. Fluid Mech. **130**, 186 (1983).
[3]C. K. K. Lun, S. B. Savage, D. J. Jeffrey, and N. Chepurnity, ''Kinetic theories for granular flow: Inelastic particles in Couette flow and slightly inelastic particles in a general flow field,'' J. Fluid Mech. **140**, 223 (1984).
[4]J. T. Jenkins and M. W. Richman, ''Grad's 13-moment system for a dense gas of inelastic spheres,'' Arch. Ration. Mech. Anal. **87**, 355 (1985).
[5]N. Sela, I. Goldhirsch, and S. H. Noskowicz, ''Kinetic theoretical study of a simply sheared two dimensional granular gas to Burnett order,'' Phys. Fluids **8**, 2337 (1996).
[6]N. Sela and I. Goldhirsch, ''Hydrodynamic equations for rapid flows of smooth inelastic spheres, to Burnett order,'' J. Fluid Mech. **361**, 41 (1998).
[7]C. S. Campbell, ''The stress tensor for simple shear flows of a granular material,'' J. Fluid Mech. **203**, 449 (1989).
[8]C. S. Campbell and C. E. Brennen, ''Computer simulation of granular shear flows,'' J. Fluid Mech. **151**, 167 (1985).
[9]O. R. Walton and R. L. Braun, ''Stress calculations for assemblies of inelastic spheres in uniform shear,'' Acta Mech. **63**, 74 (1986).
[10]C. S. Campbell, ''Rapid granular flows,'' Annu. Rev. Fluid Mech. **22**, 57 (1990).
[11]S. B. Savage, ''Numerical simulations of Couette flow of granular materials; spatio-temporal coherence and 1/*f* noise,'' in *Physics of Granular Media*, edited by J. Dodds and D. Bideau (Nova Science, New York, 1992), pp. 343–362.
[12]M. A. Hopkins and M. Y. Louge, ''Inelastic microstructure in rapid granular flows of smooth disks,'' Phys. Fluids A **3**, 47 (1991).
[13]I. Goldhirsch and G. Zanetti, ''Clustering instability in dissipative gases,'' Phys. Rev. Lett. **50**, 1619 (1993).
[14]O. R. Walton, H. Kim, and A. Rosato, ''Micro-structure and stress differences in shearing flows,'' in *Mechanics Computing in the 1990's and Beyond*, edited by H. Adeli and R. L. Sierakowski (ASCE, 1991), Vol. 2, pp. 1249–1253.
[15]S. B. Savage, ''Instability of unbounded uniform granular flow,'' J. Fluid Mech. **241**, 109 (1992).
[16]C. Babic, ''On the stability of rapid granular flows,'' J. Fluid Mech. **254**, 127 (1993).
[17]P. J. Schmid and H. K. Kytomaa, ''Transient and asymptotic stability of granular shear flow,'' J. Fluid Mech. **264**, 255 (1994).
[18]C.-H. Wang, R. Jackson, and S. Sundaresan, ''Stability of bounded rapid shear flows of a granular material,'' J. Fluid Mech. **308**, 31 (1996).
[19]M. Alam and P. R. Nott, ''The influence of friction on the stability of unbounded granular shear flow,'' J. Fluid Mech. **343**, 267 (1997).
[20]S. McNamara and W. R. Young, ''Inelastic collapse and clumping in a one dimensional granular medium,'' Phys. Fluids A **3**, 47 (1993).
[21]V. Kumaran, ''Asymptotic solution of the Boltzmann equation for shear flow of smooth inelastic disks,'' Physica A **275**, 283 (2000).
[22]V. Kumaran, ''Anomalous behavior of hydrodynamic modes in the two dimensional shear flow of a granular material,'' Physica A **284**, 246 (2000).
[23]P. Resibois and M. de Leener, *Classical Kinetic Theory of Fluids* (Wiley, New York, 1977).
[24]B. Kamgar-Parsi and E. G. D. Cohen, ''Eigenmodes of a dilute simple gas in equilibrium,'' Physica A **138**, 249 (1986).
[25]W. G. Vincenti and C. H. Kruger, *Introduction to Physical Gas Dynamics* (Wiley, New York, 1966).
[26]J. P. Hansen and I. McDonald, *Theory of Simple Liquids* (Academic, London, 1990).
[27]M. Lee and J. W. Dufty, ''Transport far from equilibrium: Uniform shear flow,'' Phys. Rev. E **56**, 1733 (1997).